High Power Laser Science and Engineering, (2023), Vol. 11, e70, 8 pages.
doi:10.1017/hpl.2023.61

HIGH POWER LASER SCIENCE AND ENGINEERING

RESEARCH ARTICLE

A 115 ps, 100 Hz high-beam-quality laser based on transient stimulated Brillouin scattering pulse compression

Jianfeng Yue[1,2], Yulei Wang[1,2], Mengyu Jia[1,2], Kai Li[1,2], Chen Cao[1,2], Yu Yu[1,2], Yunfei Li[1,2], and Zhiwei Lü[1,2]

[1] *Center for Advanced Laser Technology, Hebei University of Technology, Tianjin, China*

[2] *Hebei Key Laboratory of Advanced Laser Technology and Equipment, Tianjin, China*

(Received 16 March 2023; revised 9 July 2023; accepted 21 July 2023)

Abstract

This work demonstrates the generation of short pulse duration and high-beam-quality laser pulses using transient stimulated Brillouin scattering at a high repetition rate. Thermal effects and optical breakdown are identified as the main factors that restrict energy reflectivity and beam quality under high repetition rates and transient situations. Through experimental analysis, the interaction length and focal point size are determined to be the key parameters in reducing the thermal effect by reducing the absorption of the laser pulse by the medium. The obtained results show that pulses with a duration of 175 ps and beam quality M^2 of around 1.2 can be achieved with a maximum energy reflectivity of over 40% under an interaction length of 50 mm. Furthermore, at an interaction length of 90 mm, a pulse output with a minimum duration of 115 ps ($0.5\tau_Q$) is achieved.

Keywords: high beam quality; high energy; nonlinear optics; stimulated Brillouin scattering

1. Introduction

A laser system with a high repetition rate, excellent beam quality and hundreds of picosecond pulses has immense potential in various applications, such as laser processing[1–3], medical aesthetics[4,5] and Thomson scattering diagnostics[6]. Stimulated Brillouin scattering (SBS), a third-order nonlinear phenomenon, is often utilized in laser systems for phase conjugation and pulse compression[7]. The stimulated Brillouin scattering phase conjugate mirror (SBS-PCM) is capable of correcting static and dynamic wavefront distortion caused by thermal effects when integrated with a master-oscillator power amplifier[8–11]. However, to achieve high compensating effects, the Stokes pulse fidelity must be strictly maintained. The fidelity of the Stokes pulse is directly linked to the energy reflectivity and is sensitive to the slope of the pump pulse rise time. Under transient conditions, when the rise time of the pump pulse is less than the dielectric phonon lifetime, the ability to discriminate between conjugate modes in the SBS process[12,13] is reduced. As a result, the fidelity at low energy reflectivity is low and unstable, limiting the application of the SBS-PCM in short pulse duration laser systems. However, our research findings indicate that even if the pump pulse spot is distorted during transient SBS, the Stokes pulse can still maintain a good spot shape without requiring a secondary pass through the distortion medium. Furthermore, transient SBS can produce pulse outputs of 100 picoseconds (ps) or less in duration. Thus, a comprehensive study of transient SBS is necessary to achieve laser pulses with high beam quality and short pulse durations.

However, it is worth noting that most of the research work in this field has focused on pulse compression. The aim is to obtain shorter pulse durations, which are theoretically limited to one-quarter of the medium's oscillation period (τ_Q, equal to $1/(4\Omega_B)$, where Ω_B is the Brillouin frequency shift)[14]. For example, de Saxcé and Picart[15] used two-stage compression to produce pulse outputs with pulse durations of 252 ps, where the second-stage transient SBS energy reflectivity was 32%; Wang *et al.*[16] achieved a 60 ps pulse output at the frequency-doubled light using transient SBS, but neither broke τ_Q. When the fundamental light was used

Correspondence to: Yulei Wang, Center for Advanced Laser Technology, Hebei University of Technology, Tianjin 300401, China. Email: wyl@hebut.edu.cn

as the pump, the energy reflectivity was found to be less than 20%. With respect to the results that show pulse durations less than τ_Q, Liu *et al.*[17] obtained pulse outputs of average duration close to τ_Q in the new liquid medium PF-5060, where the shortest pulse duration measured was $0.88\tau_Q$, with an energy reflectivity of around 30%. In the same year, Cao *et al.*[18] also obtained a pulse output with a duration of less than τ_Q at a repetition frequency of 200 Hz and an energy efficiency of less than 40%. While the research on transient SBS pulse compression is developing rapidly, little is known about aspects such as the energy reflectivity of transient SBS, particularly with regard to spot profiles.

To achieve high beam quality and energy reflectivity through high repetition rate transient SBS, several challenges must be overcome. These challenges include thermal effects resulting from laser field absorption by impurities, optical breakdown of the SBS medium and low gain of transient SBS. When intense laser pulses propagate through a medium, impurity molecules within the medium can absorb the optical energy and convert it into heat. At high peak powers, the accumulated heat from impurity absorption results in a rapid increase in the temperature of the medium, leading to thermal defocusing and focal spot distortion. The enlarged beam size at the focus reduces the intensity and excites an uneven phonon field, thereby impacting the efficiency and performance of SBS compression or amplification processes and decreasing the SBS reflectivity. As the temperature further increases, electrons in the impurities become excited, generating free electrons and resulting in local ionization and electron dissociation, leading to the formation of high-density free carriers. These free carriers, under the influence of the intense laser field, accelerate and collide with other molecules, further enhancing the local temperature and energy density. Ultimately, this can lead to optical breakdown of the medium, involving the rupture and ionization of chemical bonds[19]. Compared to other media, perfluorocarbon compounds have all the hydrogen atoms attached to carbon atoms replaced by fluorine atoms. Fluorine has the highest electronegativity, and the carbon–fluorine bond possesses significant bond energy (5.6 eV). Therefore, low-absorption and large bond energy perfluorocarbon compounds are employed in high-power SBS systems[20]. Recent studies have demonstrated that microfiltration of the medium is an effective method for reducing the heat effect[21].

Regarding the low gain of transient SBS, it is worth noting that the gain coefficient (g) of SBS is inversely proportional to the laser beam linewidth, which is broad in transient SBS[22]. In addition, due to the speed at which the phonon field builds up, the pump pulse front has already passed through the generated area before the Stokes pulse can extract its energy. These two factors contribute to the low energy reflectivity of transient SBS. To overcome the low gain in transient SBS, the selection of an appropriate medium is crucial. It should possess a shorter phonon lifetime to facilitate the rapid establishment of the phonon field and its prompt response to laser pulses. In addition, a higher gain coefficient is desirable to enable efficient extraction of laser pulse energy once the phonon field is established. This combination can enhance the efficiency of SBS in practical applications.

In this study, our focus is on developing a transient single-cell SBS system that can provide high-beam-quality laser output at high reflectivity. We achieve this by utilizing 3M electronic-fluoride fluid FC-770. Our experiments demonstrate the generation of output laser pulses at a repetition rate of 100 Hz, with a beam quality of $M^2 = 1.14$. Furthermore, we have produced pulse output with a maximum energy reflectivity exceeding 40% and an average pulse length of $0.83\tau_Q$. Due to the attenuated thermal effects in the medium, the focused region has a higher power density, which enables the Stokes pulse to extract energy fully from the pump pulse. We believe that this is a pioneering experiment, and the outcomes will guide new and later SBS research work.

2. Experimental setup

A schematic diagram of the experimental setup is shown in Figure 1. The pump source is composed of a single longitudinal mode microchip laser and a double-stage amplifier. The

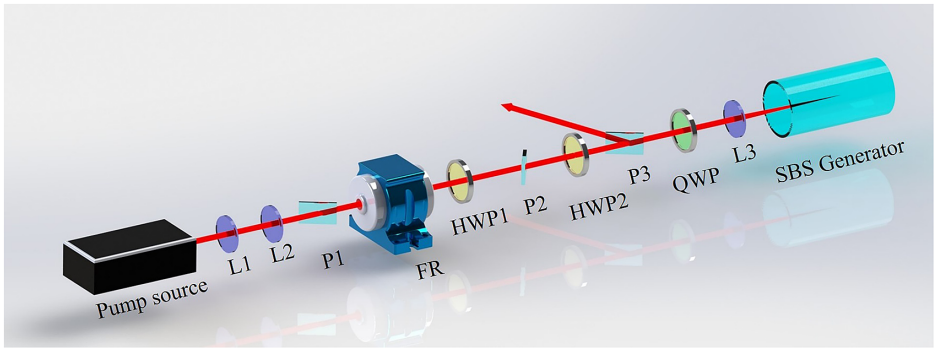

Figure 1. Schematic diagram of the experimental setup. FR, Faraday rotator; P, polarizer; HWP, half-wave plate; QWP, quarter-wave plate; F, lens; M, reflector.

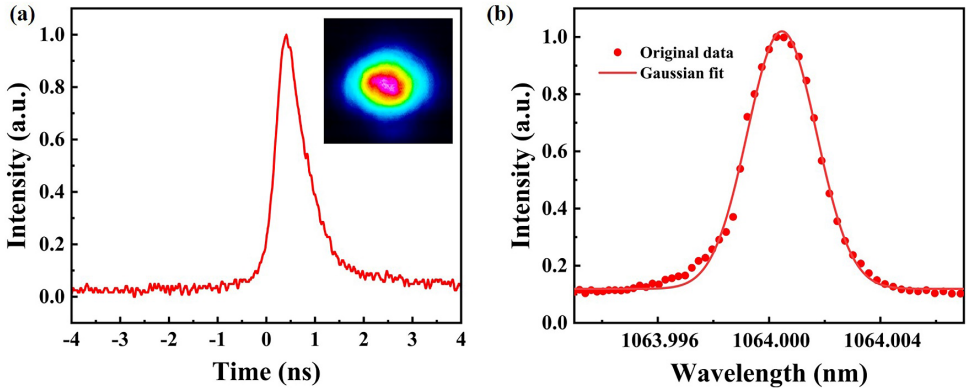

Figure 2. Pump pulse parameters: (a) typical time domain waveform and output spot of the pump pulse; (b) pump pulse linewidth.

former has a wavelength of 1064 nm, an output energy of 70 mJ and a repetition rate of 100 Hz. A typical pump pulse time domain waveform and the spatial distribution are given in Figure 2(a), with a pulse duration of 720 ps and slight distortion in the spatial profile. A Fabry–Pérot interferometer (a line width measurement device based on parallel plate equal to inclination interference) was used to measure the linewidth of the seed source, shown in Figure 2(b), and the result was 900 MHz[23]. The divergence angle of the laser beam was decreased using a collimation system made up of lenses L1 and L2. A Faraday rotator (FR), polarizers P1 and P2 and a half-wave plate (HWP) are used as isolators since the backscattered light might harm the pump source. Half-wave HWP2 and polarizer P3 regulate the pumping pulse energy into the SBS medium cell. The pump pulse travels through the quarter-wave plate and is focused by L3 into the SBS generator.

When the pump intensity in the focused region exceeded the threshold for SBS generation, the SBS-phonon field of frequency Ω_B was established due to the electrostriction action of the medium, and the pump field was quickly scattered. Through the phonon field, scattered Stokes light extracts the energy of the pump pulse. The laser beam is converted into S-polarization twice through the quarter-wavelength QWP and output at P3. The medium in the cell is FC-770, which has a high capacity, and some of the parameters are listed in Table 1. Based on previous studies[17,18], achieving both narrow pulse width and high reflectivity in SBS systems is challenging due to the trade-off between high gain and short phonon lifetime. Both factors play crucial roles in SBS performance. Therefore, in this study, we selected FC-770 as the working medium. FC-770 possesses a shorter phonon lifetime compared to PF-5060 and higher gain compared to HT-230, while also exhibiting a high breakdown threshold. This choice was made to strike a balance between these important parameters and optimize the SBS performance. The medium is filtered many times using a filter membrane (polycarbonate track etch (PCTE), GVS) with a pore size of 10 nm in order to guarantee that it is as clean as possible.

Table 1. Compilation of relevant parameters of the SBS-active media used in this work (values are remeasured and calculated for the media at a temperature of 23°C).

Medium	Refractive index n	Kinematic viscosity η (mm^2/s)	Phonon lifetime τ_B (ps)	Brillouin shift Ω_B (MHz)	Quarter acoustic wave oscillation period τ_Q (ps)
FC-770	1.27	0.66	682.4	1081	231.27

The temporal characteristics of the laser beam are measured by combining a rapid photodetector (UPD-35-UVIR-D, Alphalas GmbH, Germany; rise time <35 ps) with a digital oscilloscope (DPO71254C, Tektronix, USA; bandwidth 12.5 GHz; sampling rate 100 Gsamples/s). The laser pulse energy was measured by an energy meter (Vega Pyroelectric PE50DIF-ER (s/n:917609), Ophir Optronics, Israel).

3. Results and discussion

The interaction length L_S is defined as the length of the pump pulse that passes through the medium, as shown in Figure 3. The theoretical optimum interaction length is calculated using the formula $L_{th} = c\tau_P/2n$[24], where c

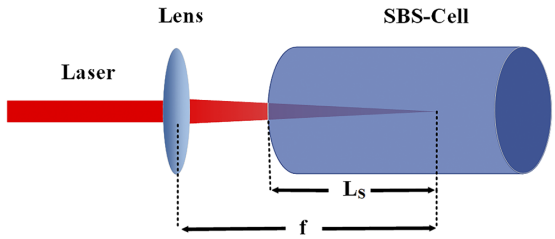

Figure 3. Interaction distance diagram, where L_S is the interaction length and f is the focal length of the lens.

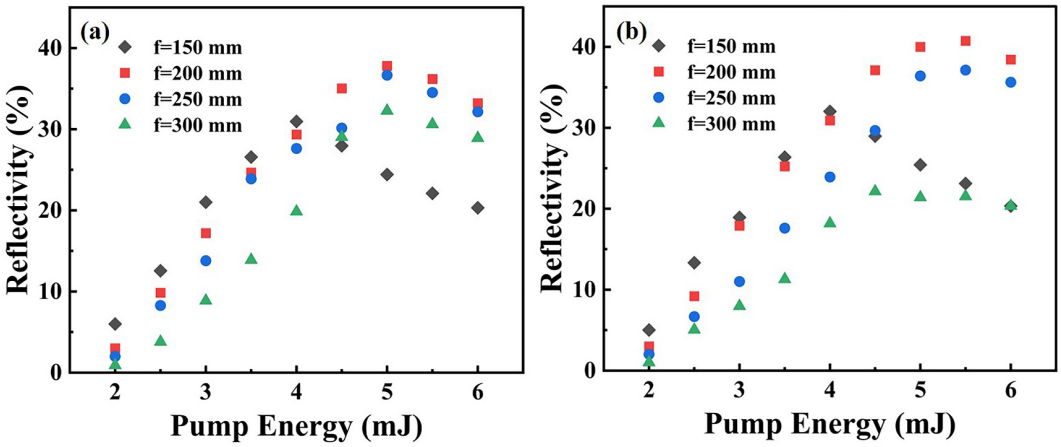

Figure 4. Relationship between energy reflectivity and pump energy at different focal lengths: (a) interaction length 90 mm; (b) interaction length 50 mm.

represents the speed of light, τ_P denotes the duration of the pump pulse and n signifies the refractive index of the SBS medium. By adjusting the distance between the lens and the SBS cell, the interaction length can be controlled. For this study, the theoretically optimal interaction length is approximately 90 mm.

3.1. Transient SBS energy reflectivity

The relationship between energy reflectivity and pumping energy is shown in Figure 4 for the interaction lengths of 90 and 50 mm, and various focal lengths of the lens conditions. Each data point represents an average value of 500 pulses. It is observed that as the pumping energy increases, the energy reflectivity initially rises rapidly, but then gradually decreases. In addition, the short duration of the pump pulse and the high intensity of the rising edge result in a low SBS generation threshold of approximately 2 mJ. The gain of the system can be expressed as follows:

$$G = gI_0L_S, \tag{1}$$

where I_0 represents the peak power density of the pump pulse at the focus. As the system's gain increases, the buildup rate and intensity of the phonon field also increase, leading to a quick rise in the pump field to Stokes field energy conversion efficiency. However, with the increase in thermal effect as the pump energy increases, optical breakdown occurs, resulting in severe damage to the phonon field and reduced energy reflectivity. Comparing the results of energy reflectivity at various focal lengths, it is observed that energy reflectivity rises with lower focal length. This is because the size of the focal point spot size increases with the focal length of the lens, and therefore G is inversely proportional to the focal length at the same energy. As the focal length shortens, the gain of the system increases, allowing the Stokes pulse to extract energy more efficiently.

When the focal length is reduced from 300 to 200 mm, the breakdown threshold is around 4.5 mJ, even though the power density at the waist increases. The comparison of the spatial distribution of Stokes pulses at a pumping energy of 5 mJ in Figure 5 shows that the distortion is not worse than the 3 mJ case, which also proves that the breakdown is not worse than 3 mJ case. However, when the focal length was further reduced to 150 mm, the optical breakdown threshold dropped sharply. At the pump energy of 3 mJ, we observed a significant optical breakdown in the SBS cell. Further, when the pump energy is 5 mJ, it exhibits the same characteristics as described above. The reason for this is the close relationship between optical breakdown and focal size. The smaller the focal area, the faster the energy is absorbed by impurities in the focal area. This, in turn, leads to faster heat buildup and local overheating, resulting in ionization and optical breakdown. As a consequence, the SBS process is hindered, and the scattering intensity is reduced, leading to a rapid decrease in energy reflectivity. Therefore, the focal point size must not be too small.

As depicted in Figure 4(a), we observed a decrease in energy reflectance over 5 mJ at all focal lengths, except the $f = 150$ mm case. This suggests that optical breakdown is not effectively mitigated. This is due to the fact that while the intensity at the focal point decreases, the heat absorption area expands. Consequently, the temperature difference between the center and its surroundings decreases, and the heat does not spread efficiently. As a result, optical breakdown can still occur under high peak power conditions, and the increase in focal point size can lead to a reduction in G and a decrease in reflectivity. So, selecting an appropriate focal spot size in transient SBS experiments can improve both the breakdown threshold and energy reflectivity.

The graph in Figure 6 displays the relationship between output energy and pump energy for different interaction lengths, with a focal length of 200 mm. Each data point represents the average of 500 pulses, and to illustrate the stability of the output energy, the square root of the variance

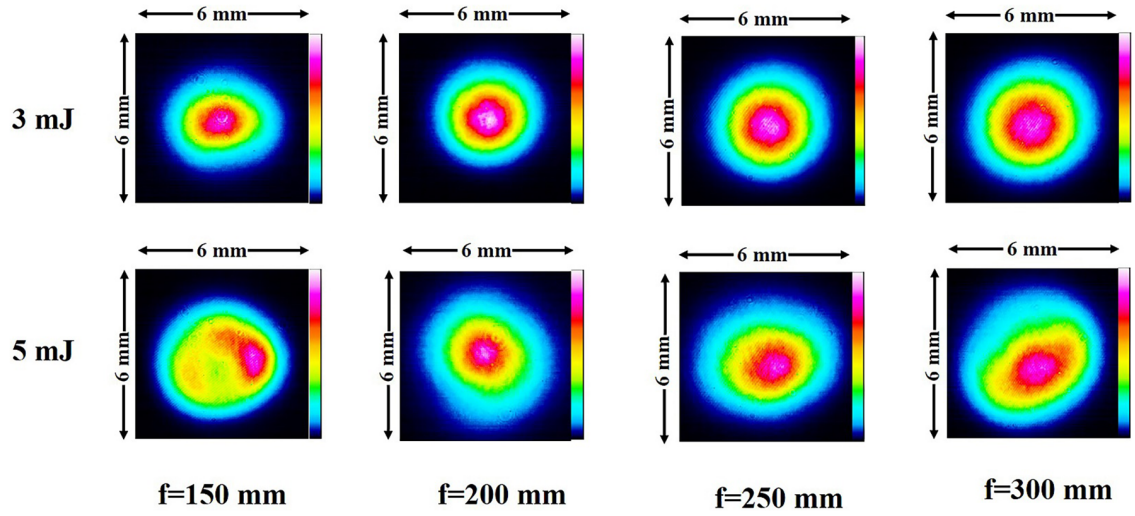

Figure 5. At the interaction length of 90 mm: the spatial profile of Stokes pulses at different focal lengths with pump energies of 3 and 5 mJ, respectively.

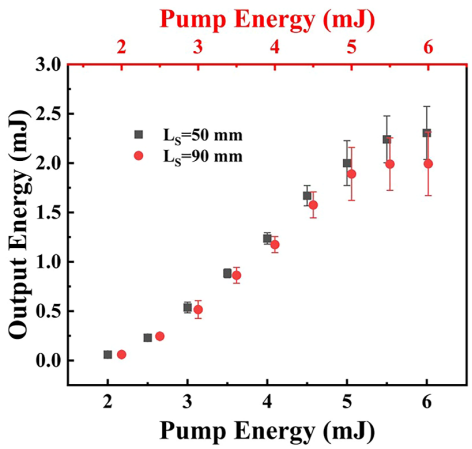

Figure 6. With a focal length of 200 mm, output energy as a function of pump energy at different interaction lengths.

(standard deviation) was calculated and added as an error bar. The reflected energy initially increases sharply but then slows down as the pumping energy increases. From the graph, we can infer that with shorter interaction lengths, the system gain decreases, but both output energy and stability increase. Therefore, a shorter interaction length results in higher stability and greater output energy.

This behavior is due to thermal effects, which become more severe with longer interaction lengths. Figure 7 depicts the spatial distribution of Stokes pulses, revealing that distortion due to thermal effects is more pronounced with longer interaction lengths. This explains why energy reflectivity decreases with high energies and long interactions. Figure 8 displays the spot diameters (full width at $1/e^2$ of the maximum intensity) of the Stokes pulses at different pump energies (the measurement position is located around 100 mm from the polarizer P3). The cross-field size of the Stokes pulse is more stable with the shorter interaction lengths.

As the interaction length decreases, the stability of the output energy and spatial distribution increases, due to weakening of the thermal effect. Our analysis indicates that thermal convection occurs anywhere the laser pulse passes, especially at high repetition frequencies. Therefore, the longer the interaction length, the more severe the thermal effect becomes, but the interaction length is limited by the damage threshold of the front window mirror and cannot be made infinitely short.

Furthermore, Figure 4 shows that at a focal length of 300 mm, the energy reflectivity is significantly reduced at an interaction length of 50 mm compared to an interaction length of 90 mm. This is because the scattering intensity is too weak due to the fact that the system gain (G) is too small. Therefore, the appropriate interaction length should be chosen according to the size of the focal point. In our experiment, the focal point size was 175 μm and the interaction length was 50 mm. We plan to design a special experiment in the future to further explore the relationship between the interaction length and focal point size.

3.2. Transient SBS pulse compression

SBS pulse compression arises from the asymmetric amplification of the leading and trailing edges of Stokes pulses. Figure 9(a) illustrates the relationship between the output pulse duration and pump energy when the interaction length is 90 mm. As the pump energy increases, the rising edge of the Stokes pulse extracts energy until the saturation point is reached, resulting in a minimum pulse duration. Subsequently, with a further increase in pump energy, some of the energy is transferred to the trailing edge, leading to a reduction in the asymmetry between the leading and trailing edges and an increase in pulse duration.

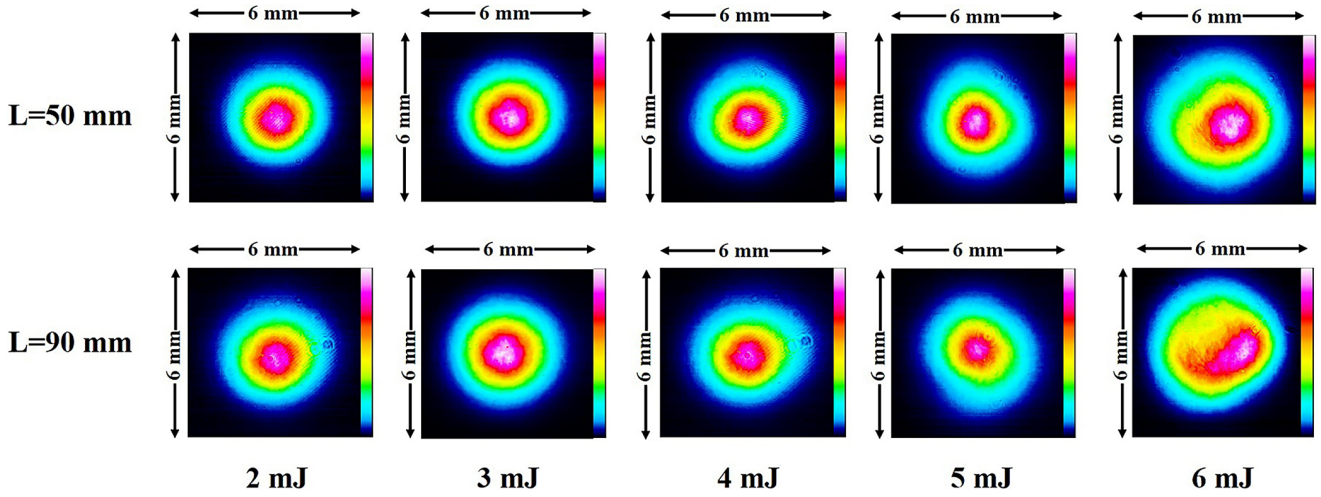

Figure 7. With a focal length of 200 mm, the typical spatial profile of Stokes pulses at different pump energies for interaction lengths of 50 and 90 mm, respectively.

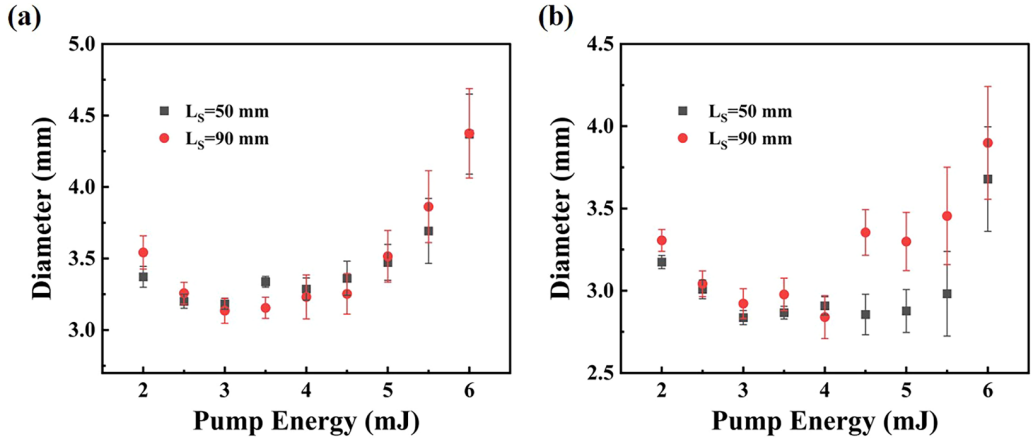

Figure 8. With a focal length of 200 mm, the diameter of spot versus pump energy for different interaction lengths: (a) diameter in the *x*-axis direction; (b) diameter in the *y*-axis direction.

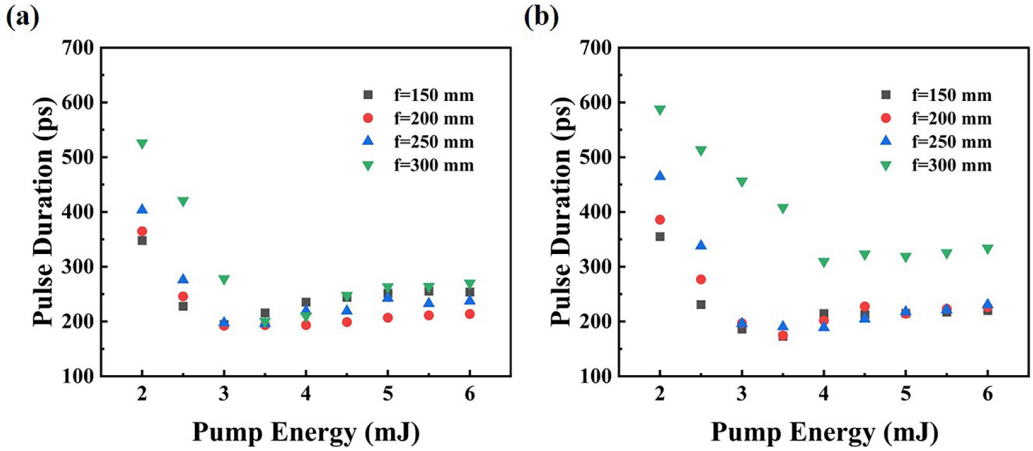

Figure 9. With different focal length conditions: (a) interaction length of 90 mm; (b) interaction length of 50 mm.

When comparing the pump energy required to obtain the shortest pulse duration at different focal lengths, it is observed that the longer the focal length, the more power is required. This is due to the fact that a larger focal length gives a larger focal spot to reduce the scattering intensity, so that the gain of the system decreases according to Equation (1). Consequently, more pumping energy is required to extract sufficient energy for the rising edge of the Stokes pulse.

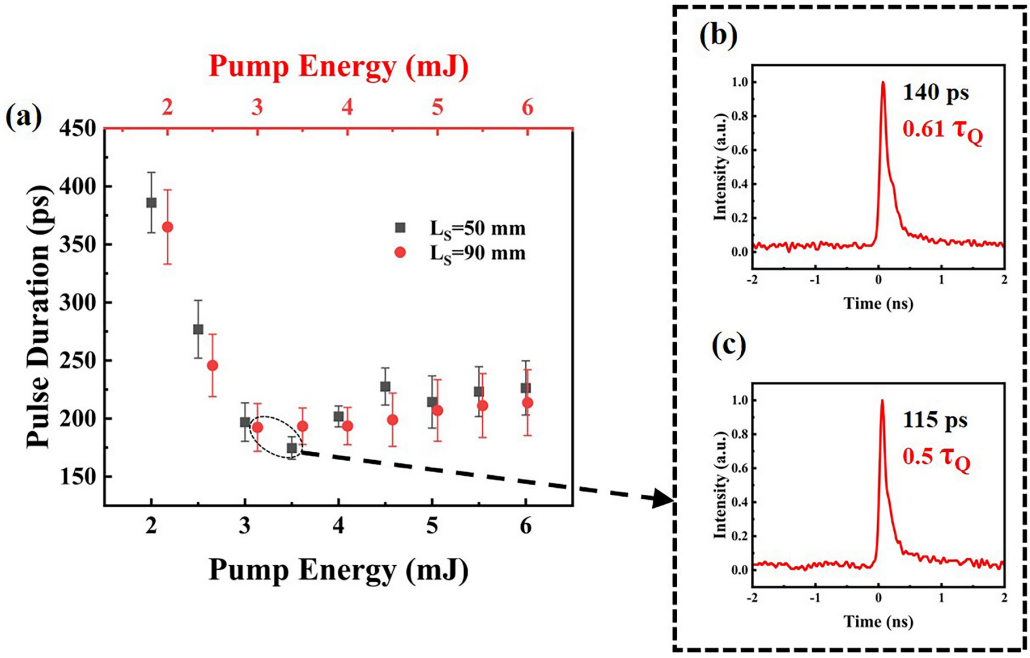

Figure 10. Output pulse duration characteristics at the focal length of 200 mm: (a) output pulse duration versus pump energy for different interaction lengths; (b), (c) output pulse waveforms with the shortest duration for interaction lengths of 50 and 90 mm, respectively.

Figure 9(b) illustrates the variation of the output pulse duration with pumping energy for an interaction length of 50 mm. As the interaction length decreases, the minimum pulse duration becomes shorter but more pumping energy is required. However, when the focal length is 300 mm, the Stokes pulse does not extract the pumping energy efficiently, resulting in an increase in pulse duration as the interaction length is reduced.

On the other hand, as the interaction length decreases, the stability of pulse duration increases, as shown in Figure 10, which shows the relationship between pulse duration and pump energy for different interaction lengths at a focal length of 200 mm. A shorter interaction length leads to higher stability and smaller average pulse durations. The shortest observed pulse duration is shown in Figure 10(b), with the smallest mean pulse duration being 175 ps ($0.75\tau_Q$). It is worth noting that a minimum pulse duration of 115 ps was recorded at an interaction length of 90 mm. Thus, the longer interaction length of the high-frequency transient SBS favors pulse compression, but thermal effects reduce the temporal and spatial stability of the SBS and increase the mean pulse duration.

The output Stokes beam profile has a good shape and a consistent energy distribution when the interaction length is 50 mm and the pump energy is 3.5 mJ, and the measured beam qualities are $M_x^2 = 1.133$ and $M_y^2 = 1.147$, as shown in Figure 11. In order to achieve pulses with improved beam quality and shorter pulse durations, additional research is required to investigate strategies for reducing thermal effects.

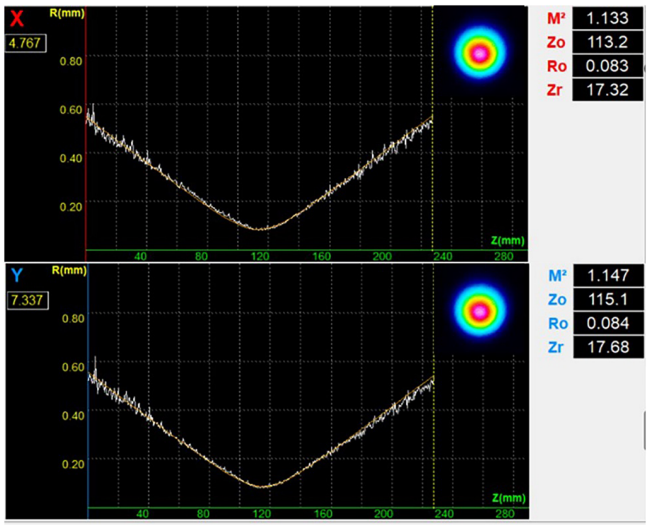

Figure 11. Stokes beam quality M^2 and spatial profile at pump energy of 3.5 mJ.

4. Conclusion

In summary, our study aimed to generate short-duration and high-beam-quality pulses using high repetition rate transient SBS. Our results demonstrated that by shortening the interaction length, the thermal effects in SBS can be significantly reduced, resulting in the more energy reflectivity, shorter pulse durations and higher stability. Specifically, at the focal length of 200 mm and the interaction length of 50 mm, the FC-770 produced a pulse with a minimum average duration

of 175 ps, a good spatial profile, no noticeable thermal effects and beam qualities of $M_x^2 = 1.133$ and $M_y^2 = 1.147$. Furthermore, we obtained the shortest pulse duration of 115 ps at an interaction length of 90 mm. As thermal effects can impact SBS, we recognize the need to explore other means to reduce these effects in our future work.

Acknowledgements

This work was supported by the National Natural Science Foundation of China (Nos. 62075056 and 61927815) and the Natural Science Foundation of Tianjin (No. 20JCZDJC00430).

References

1. W. Wei, Z. Li, H. O. Yang, X. L. Li, X. Y. Wang, and N. Li, Mater. Design **183**, 108156 (2019).
2. A. M. Wang, A. X. Feng, X. H. Gu, X. M. Pan, J. H. Yu, and Z. H. Jiang, Opt. Laser Technol. **159**, 109041 (2023).
3. B. X. Zheng, G. D. Jiang, W. J. Wang, X. S. Mei and F. C. Wang, Opt. Laser Technol. **94**, 267 (2017).
4. A. T. Taylor and E. P. C. Lai, Chemosensors **9**, 275 (2021).
5. N. P. Chan, S. G. Ho, S. Y. Shek, C. K. Yeung, and H. H. Chan, Laser Surg. Med. **42**, 712 (2010).
6. M. J. Walsh, M. Beurskens, P. G. Carolan, M. Gilbert, M. Loughlin, A. W. Morris, V. Riccardo, Y. Xue, R. B. Huxford, and C. I. Huxford, Rev. Sci. Instrum. **77**, 10E525 (2006).
7. Z. X. Bai, H. Yuan, Z. H. Liu, P. B. Xu, Q. Gao, R. J. Williams, O. Kitzler, R. P. Mildren, Y. L. Wang, and Z. W. Lu, Opt. Mater. **75**, 626 (2018).
8. T. Hatae, E. Yatsuka, T. Hayashi, H. Yoshida, T. Ono, and Y. Kusama, Rev. Sci. Instrum. **85**, 10E344(2012).
9. Z. J. Kang, Z. W. Fan, Y. T. Huang, H. B. Zhang, W. Q. Ge, M. S. Li, X. C. Yan, and G. X. Zhang, Opt. Express **25**, 6560 (2018).
10. H. L. Wang, S. Cha, J. K. Hong, Y. L. Wang, and Z. W. Lu, Opt. Express **27**, 9895 (2019).
11. K. Tsubakimoto, H. Yoshida and N. Miyanaga, Opt. Express **24**, 12557 (2016).
12. C. B. Dane, W. A. Neuman, and L. A. Hackel, Opt. Lett. **17**, 1271 (1992).
13. W. M. He, Z. W. Lu, Q. Wang, and Z. G. Ma, Acta Opt. Sin. **16**, 88 (1996).
14. I. Velchev, D. Neshev, W. Hogervorst, and W. Ubachs, IEEE J. Quantum Elect. **35**, 1812 (1999).
15. T. de Saxcé and P. Picart, Proc. SPIE **1873**, 262 (1993).
16. C. Wang, Z. W. Lu, and W. M. He, High Power Laser Part. Beams **15**, 1184 (2003).
17. Z. H. Liu, R. Fan, D. Jin, T. T. Luo, S. S. Li, Y. L. Wang, and Z. W. Lu, Opt. Express **30**, 12586 (2022).
18. C. Cao, Y. L. Wang, J. F. Yue, Z. B. Meng, K. Li, Y. Yu, Z. X. Bai, and Z. W. Lu, Opt. Express **30**, 33721 (2022).
19. H. Yoshida, V. Kmetik, H. Fujita, M. Nakatsuka, T. Yamanaka, and K. Yoshida, Appl. Opt. **36**, 3739 (1997).
20. W. L. J. Hasi, Z. W. Lu, S. Gong, S. J. Liu, Q. Li, and W. M. He, Appl. Opt. **47**, 1010 (2008).
21. S. Schiemann, W. Ubachs, and W. Hogervorst, IEEE J. Quantum Elect. **33**, 358 (1997).
22. H. L. Wang, S. Cha, H. J. Kong, Y. L. Wang, and Z. W. Lu, Opt. Express **27**, 29789 (2019).
23. X. N. Hun, Z. X. Bai, B. Chen, J. P. Wang, C. Cui, Y. Y. Qi, J. Ding, Y. L. Wang, and Z. W. Lu, Results Phys. **37**, 105510 (2022).
24. V. A. Gorbunov, S. B. Papernyi, V. F. Petrov, and V. R. Startsev, Sov. J. Quantum Electron. **13**, 900 (1983).